

Mechanism of Gram Variability in Select Bacteria

TERRY J. BEVERIDGE

Department of Microbiology, College of Biological Science, University of Guelph, Guelph, Ontario N1G 2W1, Canada

Received 21 August 1989/Accepted 30 November 1989

Gram stains were performed on strains of *Actinomyces bovis*, *Actinomyces viscosus*, *Arthrobacter globiformis*, *Bacillus brevis*, *Butyrivibrio fibrisolvens*, *Clostridium tetani*, *Clostridium thermosaccharolyticum*, *Corynebacterium parvum*, *Mycobacterium phlei*, and *Propionibacterium acnes*, using a modified Gram regimen that allowed the staining process to be observed by electron microscopy (J. A. Davies, G. K. Anderson, T. J. Beveridge, and H. C. Clark, J. Bacteriol. 156:837-845, 1983). Furthermore, since a platinum salt replaced the iodine mordant of the Gram stain, energy-dispersive X-ray spectroscopy could evaluate the stain intensity and location by monitoring the platinum signal. These gram-variable bacteria could be split into two groups on the basis of their staining responses. In the *Actinomyces-Arthrobacter-Corynebacterium-Mycobacterium-Propionibacterium* group, few cells became gram negative until the exponential growth phase; by mid-exponential phase, 10 to 30% of the cells were gram negative. The cells that became gram negative were a select population of the culture, had initiated septum formation, and were more fragile to the stress of the Gram stain at the division site. As cultures aged to stationary phase, there was a relatively slight increase toward gram negativity (now 15 to 40%) due to the increased lysis of nondividing cells by means of lesions in the side walls; these cells maintained their rod shape but stained gram negative. Those in the *Bacillus-Butyrivibrio-Clostridium* group also became gram negative as cultures aged but by a separate set of events. These bacteria possessed more complex walls, since they were covered by an S layer. They stained gram positive during lag and the initial exponential growth phases, but as doubling times increased, the wall fabric underlying the S layer became noticeably thinner and diffuse, and the cells became more fragile to the Gram stain. By stationary phase, these cultures were virtually gram negative.

For almost a century, the Gram reaction has been used to differentiate eubacteria into gram-negative and gram-positive varieties of cells. It is now apparent that the staining mechanism relies on the fundamental structural and chemical attributes of the bacterial wall (4, 9, 19). Bacteria with robust walls containing a high percentage of peptidoglycan have a greater tendency to retain the crystal violet-iodide complex and stain gram positive than do those with outer membranes and thin peptidoglycan layers, which stain gram negative (4). Yet sometimes the distinction between these two varieties of bacteria is not so clear-cut, since a select group of eubacteria can give an erratic response to the stain. This variability can be due to growth stress (e.g., unsuitable nutrients, temperatures, pHs, or electrolytes) that results in a number of nonviable, gram-negative cells in a gram-positive culture, but certain bacterial species are notorious for their gram variability even under optimal growth conditions (2). The cultures used in this study are representative of this latter group. Although they are usually considered to be gram-positive bacteria, these cultures frequently possess a proportion of gram-negative cells interspersed throughout the entire population. Often, the frequency of gram-negative cells progressively increases as exponential growth is attained and stationary phase is approached.

It is now possible to use a modified Gram stain to follow the staining reaction by electron microscopy (9). Gram's iodine solution, as a mordant, is replaced by an aqueous solution of potassium trichloro(η^2 -ethylene)-platinum(II) (potassium TPt), which complexes with the crystal violet via a metathetical anion exchange, forming a more neutral charge transfer complex with the pi bonds of the dye, which precipitate from solution and interact with similar complexes

to form large electron-dense aggregates that are visible by electron microscopy (9). This chemical complex stains the bacteria purple and interacts with both gram-positive and gram-negative bacteria exactly as does the more usual crystal violet-iodide complex of the unmodified stain (4, 9). Because platinum is a heavy metal ($Z_{Pt} = 78$), the cellular location of the staining complex can be visualized by electron microscopy, and its route in and out of cells can be seen. In addition, because platinum is not a typical element of bacteria, its energy-dispersive X-ray signal (i.e., $M_{\alpha,\beta}$ and $L_{\alpha,\beta}$ lines) can be easily deciphered in cells not contrasted by additional heavy metals (4, 9).

In this study, I used this technique to reveal the staining mechanism of 10 bacterial species from eight genera that have proven especially unpredictable with respect to their Gram-staining responses.

(Small portions of this research were reported at the 87th Annual Meeting of the American Society for Microbiology, Atlanta, Ga., 1 to 6 March 1987, and in reference 2.)

MATERIALS AND METHODS

Bacteria and growth conditions. *Arthrobacter globiformis* (ATCC 8010) and *Bacillus brevis* (ATCC 8246) were each grown in nutrient broth at 30°C. *Mycobacterium phlei* (University of Guelph strain 424; originally obtained from National Health and Welfare, Ottawa, Canada) was grown on tryptic soy broth at 37°C. *Corynebacterium parvum* (ATCC 11829; now designated as a *Propionibacterium acnes* strain [8]), *Actinomyces bovis* (ATCC 1192), *Actinomyces viscosus* (ATCC 15987), and *P. acnes* (ATCC 11827) were grown in brain heart infusion broth at 37°C. *Clostridium tetani* (ATCC 19406) and *Clostridium thermosaccharolyticum*

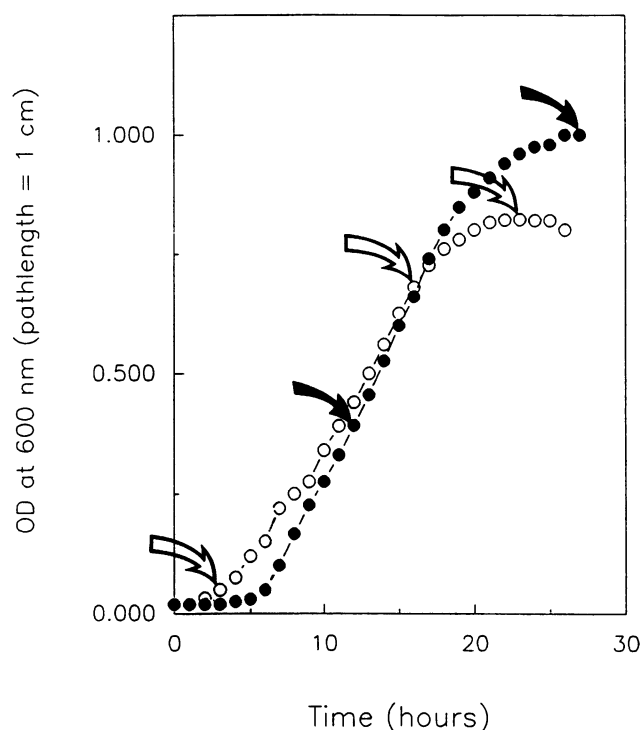


FIG. 1. Representative growth curves of two cultures used in this study. Data for *M. phlei* (●) and *Bacillus brevis* (○) are shown, as are the sampling points (arrows) used in Tables 1 and 2 for these cultures.

(ATCC 7956) were grown in prereduced thioglycolate broth at 37 and 45°C, respectively, and *Butyrivibrio fibrisolvens* (ATCC 29550) was grown at 37°C in prereduced medium M8 containing 8 g of NaHCO₃ per liter, 10 g of Casamino Acids per liter, 2.5 g of yeast extract per liter, 4 g of galactose per liter, and 20% (vol/vol) clarified rumen fluid. Cysteine hydrochloride (0.1%, wt/vol) was used as a reducing agent. All complex media were from Difco Laboratories (Detroit, Mich.), and all other chemical reagents were from Fischer Scientific Co. (Toronto, Canada).

The growth of each culture was followed by optical density at 600 nm (OD₆₀₀), using a path length of 1 cm in a Spectronic 20 (Bausch & Lomb, Inc., Ontario, Canada) so that samples could be taken at select growth phases for Gram staining and processing for electron microscopy. Cultures were grown in 250 ml of broth in 1-liter flasks on a rotary shaker. For anaerobic cultures, the flasks containing prereduced medium were first flushed with a 5% CO₂-85% N₂-10% H₂ mixture to ca. 2 atm of pressure and stoppered with neoprene plugs. Samples were taken by syringe from these cultures, using the positive pressure within the flasks to maintain anaerobiosis.

Although each culture, over time, had its own independent growth curve, mid-exponential cultures usually had OD₆₀₀ measurements ranging from 0.2 to 0.6, and OD₆₀₀ values for stationary-phase cultures ranged from 0.8 to 1.6 (the data in Fig. 1 are representative). The selection of distinct growth phases was determined by graphic analysis according to Drew (11) and Koch (17). Cultures were not grown past the maximum stationary phase (11).

Some bacteria, i.e., *M. phlei*, *A. bovis*, and *A. viscosus*, grew as flocs in fluid media, which made accurate optical density measurements difficult. In preliminary experiments,

at select growth phases, suspensions of flocs were sampled and dispersed with a Potter-Elvehjem tissue homogenizer. This produced unbroken, single-cell dispersions that could be monitored at OD₆₀₀, and the values could be accurately related to the growing broth cultures (Fig. 1 shows an adjusted *M. phlei* growth curve).

Gram stain, electron microscopy, and energy-dispersive X-ray spectroscopy (EDS). Cells taken from select growth phases were stained by both the conventional and modified regimens as outlined by Davies et al. (9). For the modified procedure, potassium TPT was synthesized from K₂(PtCl₄) and ethylene with an anhydrous SnCl₂ catalyst as described by Chock et al. (7) and was used as an aqueous 5 mM reagent to replace Gram's iodine.

Stains for light microscopy were done on heat-fixed smears of bacteria according to the following procedure. Crystal violet was used to flood the smear for 60 s, followed by flooding with an equal volume of Gram's iodine solution (conventional Gram procedure) or 50 mM TPT (TPT-modified procedure) for an additional 60 s. The mordanted stain was gently washed under running tap water (~4°C) and blotted dry with absorbant filter paper. The smears were decolorized in a slow, steady stream of hydrous 95% ethanol for 30 s and were then washed with water, blotted dry, and counterstained with carbol fuchsin for 60 s. The smears were then washed with water, blotted dry, and observed by light microscopy.

For electron microscopy and EDS, cells were harvested by centrifugation and washed twice in 50 ml of 50 mM N-2-hydroxyethylpiperazine-N'-2-ethanesulfonic acid (HEPES) buffer (pH 6.8) containing 1 mM MgCl₂. They were then put through either the conventional or TPT-modified Gram procedure as outlined above. More detail can be found in Fig. 1 of Davies et al. (9). The cells were then reequilibrated to 50 mM HEPES buffer, fixed for 1 h in 5% (vol/vol) glutaraldehyde in buffer, washed (without heavy-metal staining), and processed into Durcupan (Fluka AG, Buchs SF, Switzerland) or Epon 812 (CanEM, Guelph, Canada). From previous experience, it was found that Durcupan best preserves the TPT-crystal violet complex but is difficult to contrast with uranyl and lead once the cell preparations are sectioned. For this reason, Durcupan was used most frequently for EDS analysis, whereas Epon was used for electron microscopy.

EDS was performed on unstained thin sections, using the spectrum from the embedding resin as an index of specimen background radiation. Pt (M_{α,β} and L_{α,β}) lines were monitored for the Gram precipitate (the TPT-crystal violet complex). Spectral lines slightly upstream and downstream in the X-ray spectrum were used to establish readings of the continuum to ensure the validity of the Pt readings. Point analyses were performed on a Philips EM400T equipped with a scanning transmission electron microscope (STEM) module and an EDAX/9100/40 EDS system at 100 kV, using a spot size of 200 nm and an emission current of 80 μA. Typically, magnifications of ×280,000 and counting times of 100 to 200 s were used. When Pt distribution maps were necessary, the STEM mode was used and operated at 80 kV and 85 μA with a 50-μm condenser aperture in place. Typical magnifications in this mode were ×37,000 with scan times of 500 s.

Micrographs were taken after EDS had confirmed the presence of Pt (as TPT-crystal violet) in thin sections. These unstained sections were then counterstained with uranyl acetate and lead citrate (4) to increase contrast and to ensure the proper identification of cellular constituents. Pt could

still be identified by EDS in these sections, although overlap of the Pt and Pb lines made dot mapping difficult. Images were recorded by either a Philips EM400T or EM300 operating at 60 kV under standard conditions with a liquid nitrogen cold trap in place.

Bright-field images by light microscopy were obtained with a Zeiss photomicroscope (Universal model; Carl Zeiss, Oberkochen, Federal Republic of Germany), using a 100/1.25 oil immersion apochromatic objective lens. The images were recorded on Panatomic Plus X black-and-white film developed in D-19 (Eastman Kodak Co., Rochester, N.Y.); gram-positive cells were intensely black, whereas gram-negative cells were light gray when printed on Kodabromide F4s paper (Eastman Kodak).

RESULTS AND DISCUSSION

Light microscopy and structural attributes. The bacteria used in this study represent a group that frequently exhibits an erratic response to the Gram stain. Certainly, the list cannot be all-inclusive, but it does cover a range of 10 species representing eight genera. At the same time, it covers a range of morphotypes and physiologies. From their electron microscopic thin-section profiles, all types are considered to be gram positive in that they do not possess a lipid bilayer as an outer membrane and typically have a peptidoglycan layer that is thicker than 3.0 nm (1–3; Fig. 2 and 10). Some walls contain α -branched, β -hydroxylated acids (i.e., the mycolic acids of *M. phlei* and the corynemycolic and corynemycolenic acids of *Corynebacterium parvum* and *P. acnes* [12]), whereas others possess an additional layer above the peptidoglycan-containing matrix (i.e., the S layers of *Bacillus brevis*, *C. thermosaccharolyticum*, and *C. tetani* [20–22] and the nonperiodic layer of *B. fibrisolvens* [T. Beveridge, unpublished observations; 6]). Indeed, bacteria in this group possess a range of unique characteristics, and there is little commonality between them as distinct genera other than their gram variability. It was therefore of interest to study this phenomenon in greater detail to discover whether there was a certain unity to the mechanism of their Gram responses.

Initially, the cultures were grown in broth, sampled at distinct points in their growth curves, Gram stained by conventional means, and observed by light microscopy. Careful observations of these stains revealed that the bacteria could be divided into two distinct groups. One group, consisting of the *Actinomyces-Arthrobacter-Corynebacterium-Mycobacterium-Propionibacterium* spp., had a select population of cells (less than 30%) that were gram negative at the mid-exponential phase of growth (Table 1; Fig. 3). During the stationary phase, this percentage of the population increased but never above 40% (Table 1). The remaining group, consisting of *Bacillus-Butyrivibrio-Clostridium* spp., revealed a gradual, progressive increase toward gram negativity as the cultures aged (Table 2). Few cells were gram negative during the early growth phases (Fig. 12) but by the stationary phase, virtually the entire culture had converted (Fig. 13 and 16 [inset]; Table 2). In total, these observations were consistent for all media used in the study, divided the cultures into two staining groups, and prompted a closer look, using the modified Gram stain for electron microscopy (9).

Before the modified technique could be used for thin sections, all of the cultures were restained for light microscopy at select growth stages, using TPT to replace Gram's iodine to ensure the same gram variability as previously seen

by conventional staining; gram variability was conserved (Fig. 16 [inset]). At the same time, conventional embeddings or electron microscopy was performed to gain familiarity with the structural attributes of each bacterium under the fixation and embedding regimens used for the modified Gram stain. *A. bovis*, *A. viscosus*, *Arthrobacter globiformis*, *Corynebacterium parvum*, *M. phlei*, and *P. acnes* all possessed typical amorphous, gram-positive walls in thin section as outlined by Beveridge (1), without additional structural elements adorning their surfaces (Fig. 2 is representative). All were short rods except for the two *Actinomyces* spp., which were seen to be longer rods attached together in small chains with occasional branching, and *A. globiformis*, which was a short rod only until the late exponential growth phase, when it became a coccobacillus (no change in cell wall format was seen during this shape alteration). For this entire group of bacteria, no unusual internal structures were seen; a central fibrous nucleoid surrounded by cytoplasmic substance (mostly ribosomes) with occasional mesosomes was common (Fig. 2).

The *Bacillus brevis-B. fibrisolvens-C. tetani-C. thermosaccharolyticum* group was much different from the former group. Thin sections of these rod-shaped bacteria revealed complex wall profiles consisting of two electron-dense layers above the plasma membrane (Fig. 10 and 16 are representative). The layer immediately above the plasma membrane is the peptidoglycan-containing matrix, and the outer additional layer is a proteinaceous surface array (or S layer) (1, 21, 22). Negative stains revealed a periodicity to the additional layers of all of these bacteria except that of *B. fibrisolvens*, which appeared smooth and without a regular pattern. When thin sections of cells in early exponential growth phase were compared with those of older cells, it was apparent that the peptidoglycan-containing layer became thinner and stained more diffusely with time (cf. Fig. 17, 18, and 10 [inset]); from early exponential to stationary phase, the layer thickness typically shrank by one-half (e.g., that of *B. fibrisolvens* went from 8 to 4 nm and that of *Bacillus brevis* went from 6 to 3 nm in thickness). This shrinkage was not seen with the outer, additional layer. Throughout their growth, the *Bacillus* and *Clostridium* spp. were highly motile, and flagella were frequently seen in thin section (Fig. 16), which was not the case for the *Butyrivibrio* sp. Structural features of endospore initiation were rarely encountered with the *Bacillus* and *Clostridium* spp. during the period of growth used in this study.

Modified Gram stain on the *Actinomyces-Arthrobacter-Corynebacterium-Mycobacterium-Propionibacterium* group. Cultures were sampled at select growth phases (Fig. 1), and whole mounts and thin sections were monitored for Pt as an index of gram positivity due to cytoplasmic concentrations of TPT-crystal violet. For example, when *M. phlei* was sampled at its mid-exponential growth phase, 90% of the cells were gram positive (Fig. 3 and Table 1), and these cells in thin section gave Pt intensity values by EDS of 92% (Table 1); i.e., these cells retained copious amounts of the TPT-crystal violet complex and were strongly gram positive. Indeed, so much of the staining complex was retained that it could be dot mapped by its Pt signal (Fig. 5 and 6). Yet those few cells from this culture that were gram negative at this growth stage (Fig. 3 and Table 1) were readily identified by three traits. In thin section, they had low Pt signatures (Table 1), they were in the initial phases of septation (Fig. 4), and they had large voids in their cytoplasm (Fig. 4). These traits were shared by all other genera in this group (Table 1 and Fig. 7). It appeared that if cells were undergoing the

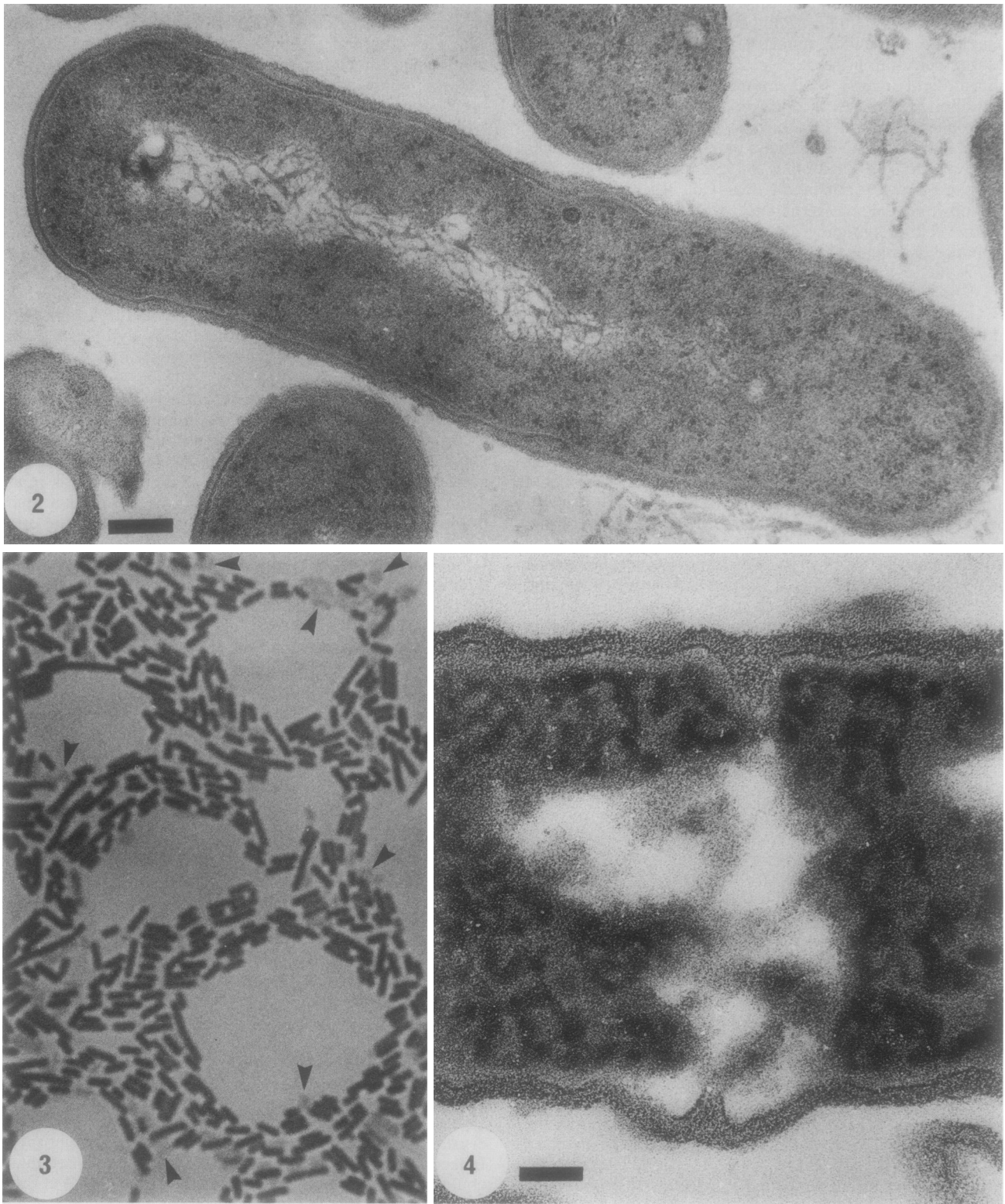


FIG. 2. Thin section of *M. phlei* from a mid-exponential growth phase that shows a cell before Gram staining. The cell wall is approximately 28 nm thick. Bar = 200 nm.

FIG. 3. Light micrograph of the cells seen in Fig. 2 after a conventional Gram stain. Most cells are darkly stained (gram positive), but the arrowheads point to those select cells that are more lightly stained (gram negative). The cells are 3 to 5 μm long.

FIG. 4. Thin section of a gram-negative cell from an *M. phlei* culture showing a septal blowout. The dark-staining material in the cytoplasm is the TPT-crystal violet complex. Bar = 100 nm.

TABLE 1. Gram reaction and TPT-crystal violet content of the gram-variable *Actinomyces-Arthrobacter-Corynebacterium-Mycobacterium-Propionibacterium* group during two growth phases

Organism	Result at given growth phase ^a									
	Mid-exponential					Stationary				
	OD ₆₀₀ ^b	% Gm+ ^c	Pt ^d	% Gm- ^c	Pt ^d	OD ₆₀₀	% Gm+	Pt	% Gm-	Pt
<i>Actinomyces bovis</i>	0.3	90	77	10	17	0.7	85	69	15	23
<i>Actinomyces viscosus</i>	0.4	85	81	15	20	1.2	70	78	30	26
<i>Arthrobacter globiformis</i>	0.4	80	67	20	20	1.5	75	62	25	21
<i>Corynebacterium parvum</i>	0.5	70	73	30	10	2.0	65	63	35	16
<i>Mycobacterium phlei</i>	0.4	90	92	10	15	1.0	85	87	15	18
<i>Propionibacterium acnes</i>	0.4	75	74	25	12	1.3	60	70	40	19

^a Gm+, Gram positive; Gm-, gram negative.^b Path length, 1 cm.^c Derived from actual Gram-stained cell counts by light microscopy and represents five different fields of view on each of two to three different stains. Each percentage was derived from ca. 500 or more cells and has been rounded to the nearest 5%.^d Derived from EDS intensity values accumulated over 120 s (live time) covering an energy range of 0 to 20 keV and presented as the percentage of Pt of the total compositional signal (i.e., Pt was ratioed against all other cellular elements that could be detected above background noise). The values represent data from the Pt M_{α,β} and L_{α,β} lines of at least 10 cells (standard deviation, <5%) and have been corrected for background emission from the plastic and grid bars. It is apparent that the major high-atomic-number element in gram-positive cells is Pt, indicative of large TPT-crystal violet deposits. Other major lines in these cells were P (nucleic acids, ribosomes, phospholipids, etc.) and C1 (a cytoplasmic electrolyte and plastic constituent). As cells became gram negative, the Pt and P signals became much reduced, and C1 approached the levels in the surrounding plastic. This indicated leakage of cellular constituents and the TPT-crystal violet complex from these cells.

initial stages of septation during division, they were unusually prone to lysis during the Gram stain. In fact, it looked as if blowouts occurred at the septal site, resulting in cytoplasmic voids as the cell substance and TPT-crystal violet leaked out (Fig. 4 and 7). This resulted in a select population of cells within each culture that had a low percentage of TPT-crystal violet (Table 1) and varying degrees of cytoplasm left within their interstices.

For more typical gram-positive rods, such as *Bacillus subtilis* and *Lactobacillus acidophilus*, it is not unusual for septal sites to be highly active autolytic centers during growth and division (5, 14). After all, these regions are major sites of newly incorporated wall material as the septum forms, and the growing septum will eventually become new polar ends once the daughter cells have separated (15). It stands to reason that the initial sites of septum ingrowth would be areas where new wall material is actively being melded into old wall, where the bonding may not be quite as hardy as previously, and where rupture due to osmotic or dehydration stress would most readily occur. Accordingly, during the Gram stain, these sites would be most prone to breakage, and these cells would be more apt to stain gram negative.

Certainly, most gram-positive cultures do not share the staining trait exhibited by the present group of bacteria,

since they are distinctly gram positive throughout most of their growth. It is possible that the very gram variability of the present group is actually outlining a common mechanistic feature of division and of the early incorporation of wall precursors at septal sites which is shared by these five genera but not with more typical gram-positive cultures.

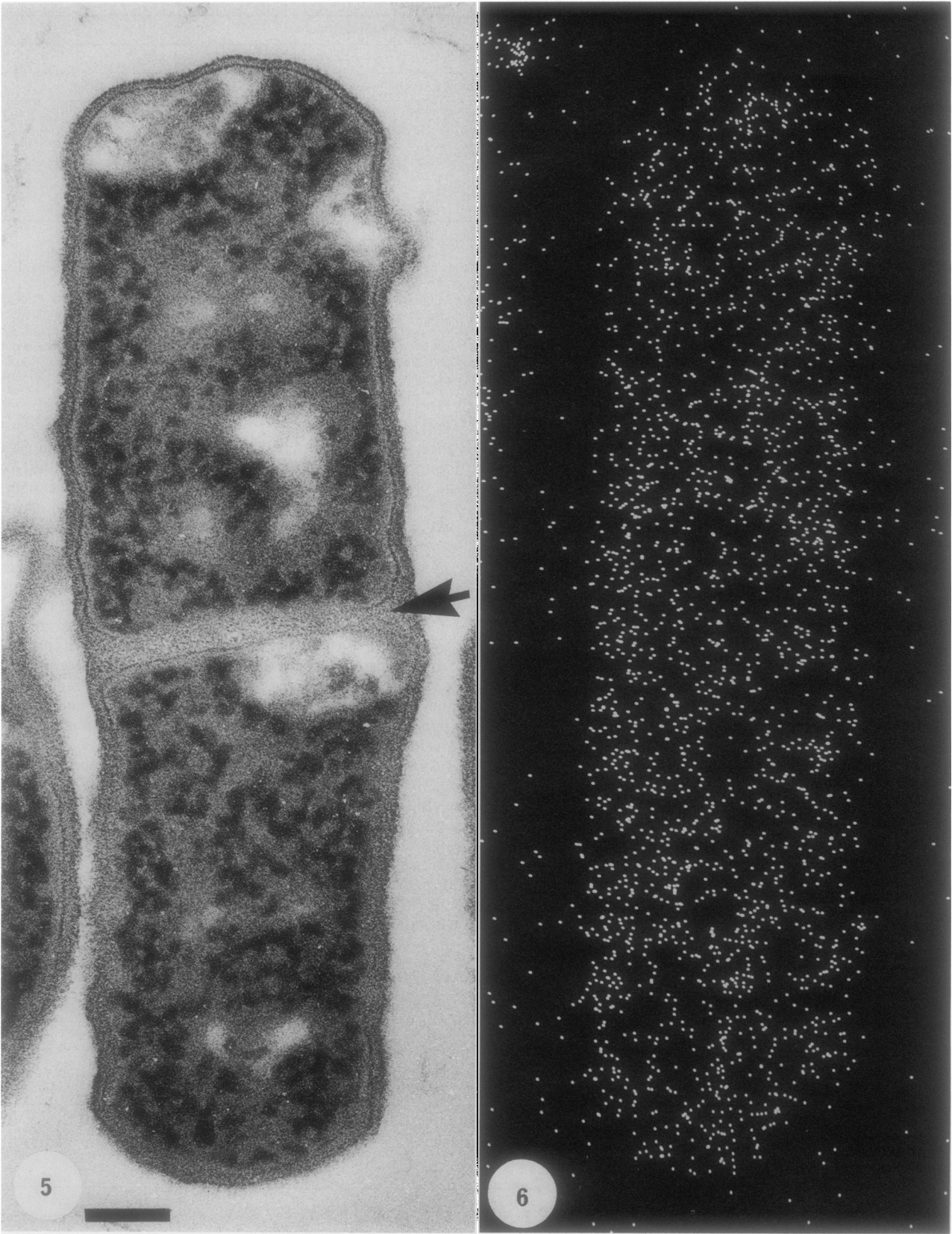
Although the numbers of gram-negative cells increased over time as the cultures entered stationary phase, these cells were still a minority (Table 1). *P. acnes* and *Corynebacterium parvum* had the highest conversion to gram negativity, and in this case an additional *modus operandi* was evident; cytoplasmic voids were not entirely confined to septation sites but could be found close to any region of the side wall (Fig. 8). Eventually, these cells lysed and became gram negative (Fig. 9). To a lesser degree, this phenomenon was also evident in the other cultures.

As cultures age and enter a stationary period, it is not uncommon for a low percentage of the cells to die and eventually lyse. I believe that this accounts for the increased gram variability seen in this group and suggest that, in addition to septal sites, certain regions of the wall in dying cells become friable and sensitive to the Gram stain. Since the polar ends have an extremely low degree of wall turnover (10), it would be the side walls of the rod that would be particularly prone to this event. Whether it was the result of

TABLE 2. Gram reaction and TPT-crystal violet content of the gram-variable *Bacillus-Butyrivibrio-Clostridium* group during growth

Organism	Result at given growth phase ^a								
	Exponential						Stationary		
	Early			Late			OD ₆₀₀	% Gm+	Pt
	OD ₆₀₀ ^b	% Gm+ ^c	Pt ^d	OD ₆₀₀	% Gm+	Pt			
<i>Bacillus brevis</i>	0.1	100	70	0.7	60	44	0.8	10	5
<i>Butyrivibrio fibriosolvens</i>	0.1	95	71	0.3	40	22	0.7	5	0
<i>Clostridium tetani</i>	0.1	95	79	0.5	50	39	1.0	5	4
<i>Clostridium thermosaccharolyticum</i>	0.1	95	64	0.6	50	36	1.2	10	7

^{a-c} See footnotes a to c, Table 1.^d The conditions used were as described in footnote d, Table 1. The standard deviation between cells was highly dependent on growth phase: early exponential, <10%; late exponential, <25%; and stationary, <5%. Since in this experiment both gram-positive and gram-negative cells were counted, the high standard deviation of late exponential phase reflects a high rate of transition within the cell population of this growth phase. It also accounts for an intermediate level of Pt.



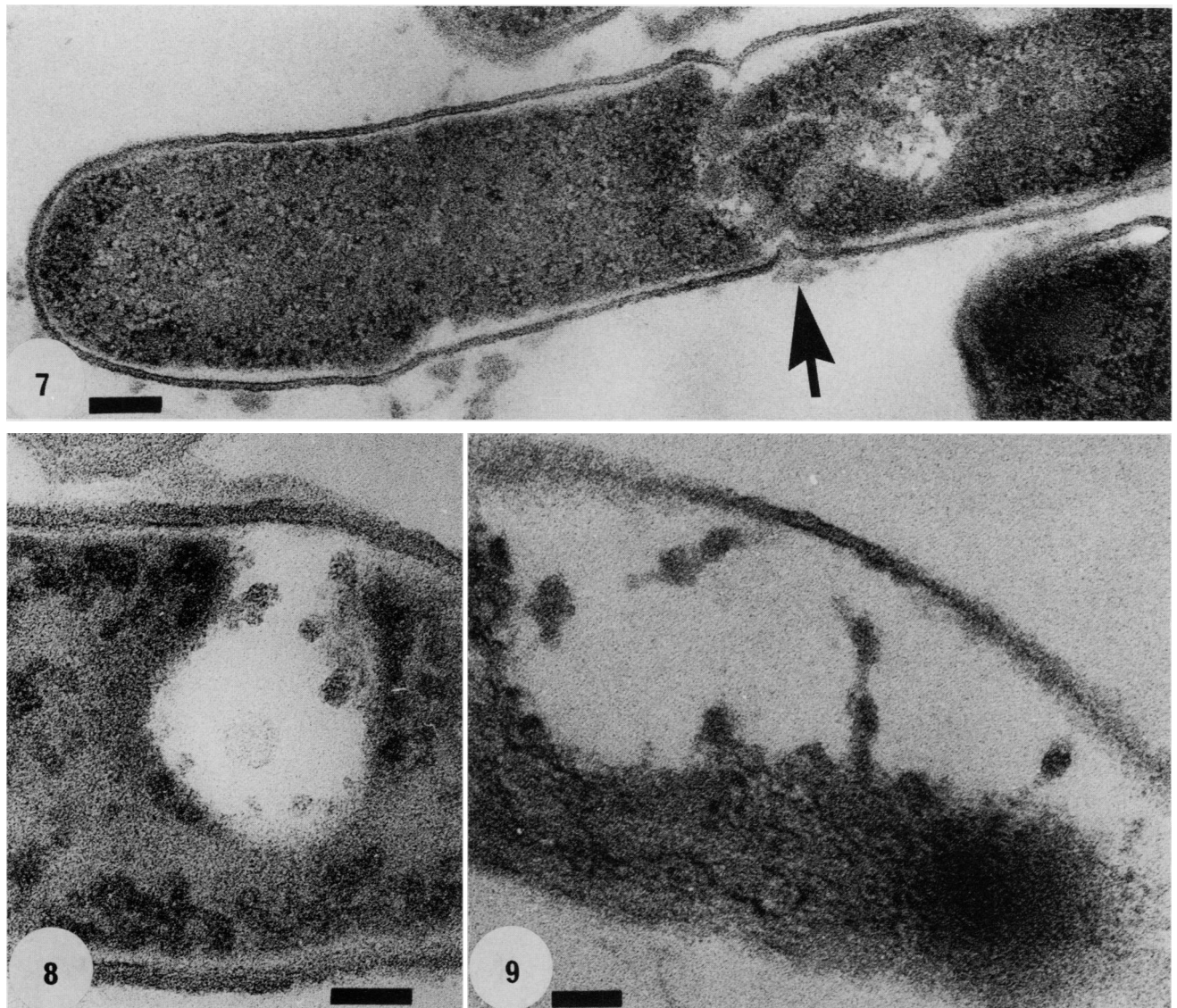


FIG. 7. Gram-stained exponential-phase *P. acnes* cell undergoing the initial stages of septation (arrow). The cell is leaking cytoplasmic substance from the division site, resulting in voids. There are few dark-staining deposits left (i.e., TPT-crystal violet), and this cell has become gram negative. The cell wall is approximately 25 nm thick. Bar = 200 nm.

FIG. 8. Part of a *P. acnes* cell from an early-stationary-phase culture. A cytoplasmic void has occurred near the wall of a nondividing cell. Bar = 100 nm.

FIG. 9. Similar to Fig. 8, but from a more advanced stationary phase. The cell has little cytoplasm left and is gram negative. Bar = 100 nm.

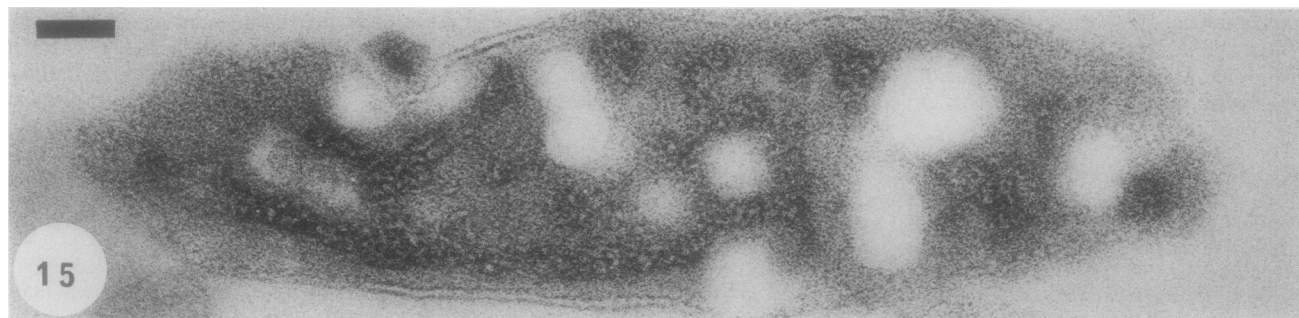
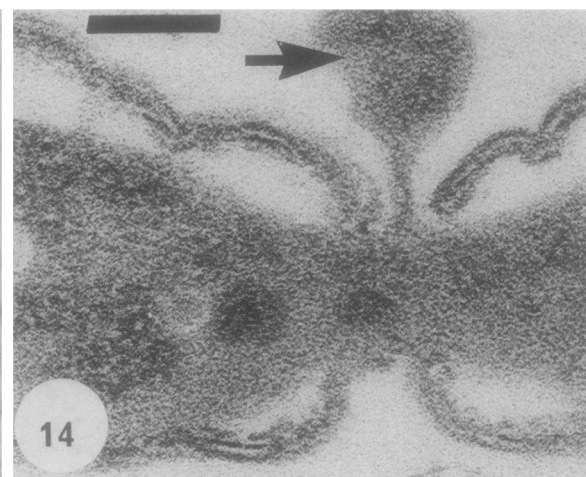
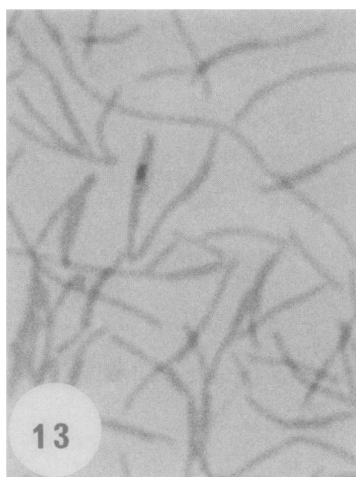
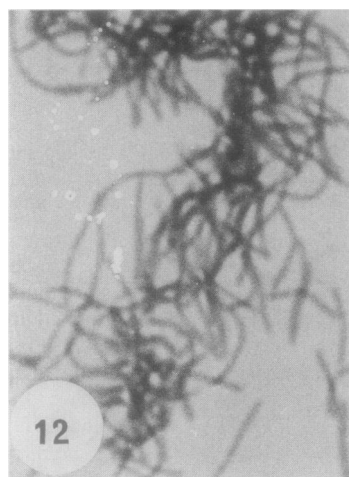
a septum blowout or a lysis point, these stationary cells would be leached of their TPT-crystal violet during decolorization and would stain gram negative.

Modified Gram stain on the *Bacillus-Butyrivibrio-Clostridium* group. Throughout the growth curves of these bacteria

(that of *Bacillus brevis* in Fig. 1 is representative), there was a steady, progressive increase in the number of cells that became gram negative (cf. Fig. 12 and 13; Table 2), so much so that at the stationary phase, virtually the entire culture had converted (Fig. 13 and 16 [inset]). Viable counts of

FIG. 5. Thin section of an *M. phlei* cell containing enough TPT-crystal violet complex (darkly stained regions in cytoplasm) to make it gram positive. Since the septum (arrow) is intact, there has been no blowout, but some cytoplasmic voids, a result of the processing, are seen. This thin section has been stained with uranyl acetate and lead citrate to heighten the contrast of the cellular structures to make them easier to distinguish. Bar = 200 nm.

FIG. 6. EDS platinum dot map of an uncontrasted cell similar to the one seen in Fig. 5. The highest concentration of dots lies within the borders of the cell, which is rod shaped, and is due to the retention of the TPT-crystal violet complex within the cytoplasm. Magnification is the same as in Fig. 5.



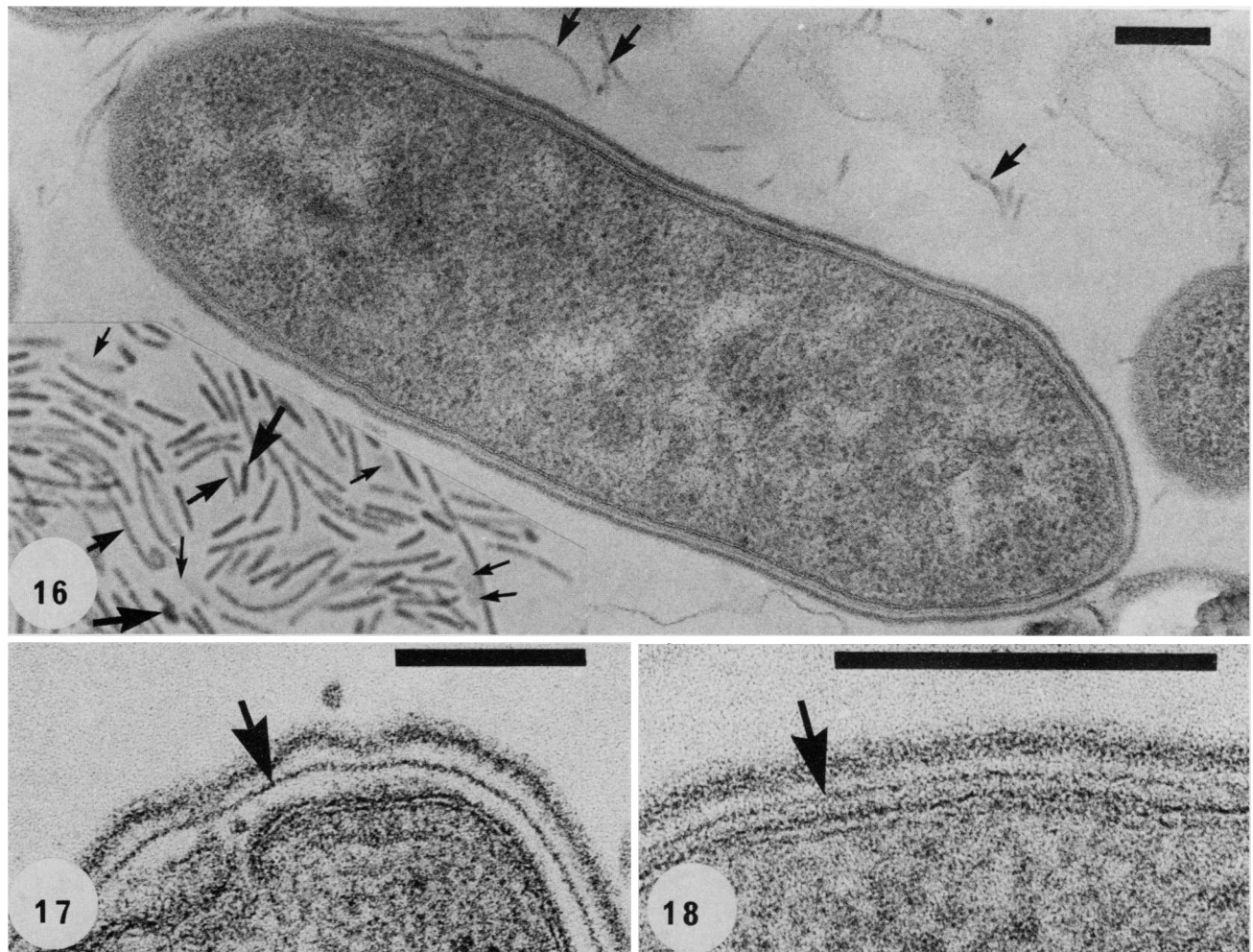


FIG. 16. Thin section of a *Bacillus brevis* cell from a culture in late exponential growth phase before Gram staining. Arrows point to some of the flagella surrounding the cell. Bar = 200 nm. The inset (lower left) is a bright-field light micrograph of the late-exponential-phase culture stained by the modified Gram stain. There is a gradation of staining intensity; some cells are definitely gram positive (large arrows), some are gram negative (small arrows), and others are in between (medium arrows). Several of the gram-negative cells have rounded up (e.g., those at the right side of the inset that are pointed to by small arrows). Cell diameter of the rods is 0.7 μ m.

FIG. 17. Thin section of the cell envelope of an early-exponential-phase *Bacillus brevis* culture. The peptidoglycan-containing layer (arrow) is 6.0 nm, and the S layer lies above it. Bar = 200 nm.

FIG. 18. Same as Fig. 17 but from a stationary-phase cell. The peptidoglycan-containing layer (arrow) is not as intensely staining and is now only 3.0 nm thick. (To make this layer more easily seen, this figure is two times the magnification of Fig. 17.) Bar = 200 nm.

bacteria (data not shown) and a survey of each growth phase by electron microscopy (Fig. 10 and 16) suggested that this increase was not entirely due to cell lysis. In general, lysis did not affect more than 5 to 10% of the culture until well into the stationary phase.

The steady increase in gram variability during growth was substantiated by a concomitant decrease in the Pt (TPT-crystal violet) signal by EDS (Table 2). Early-exponential-phase cells had so much precipitate within them that it was easily seen in thin section (Fig. 11). As growth continued, an

FIG. 10. Early-exponential-phase *B. fibrisolvens* cell before Gram staining. Bar = 100 nm. Note the difference between this cell wall and those of *M. phlei* (Fig. 2) and *P. acnes* (Fig. 7). The inset reveals this difference better and shows a two-layered wall (an arrow points to each layer). Bar of inset = 50 nm.

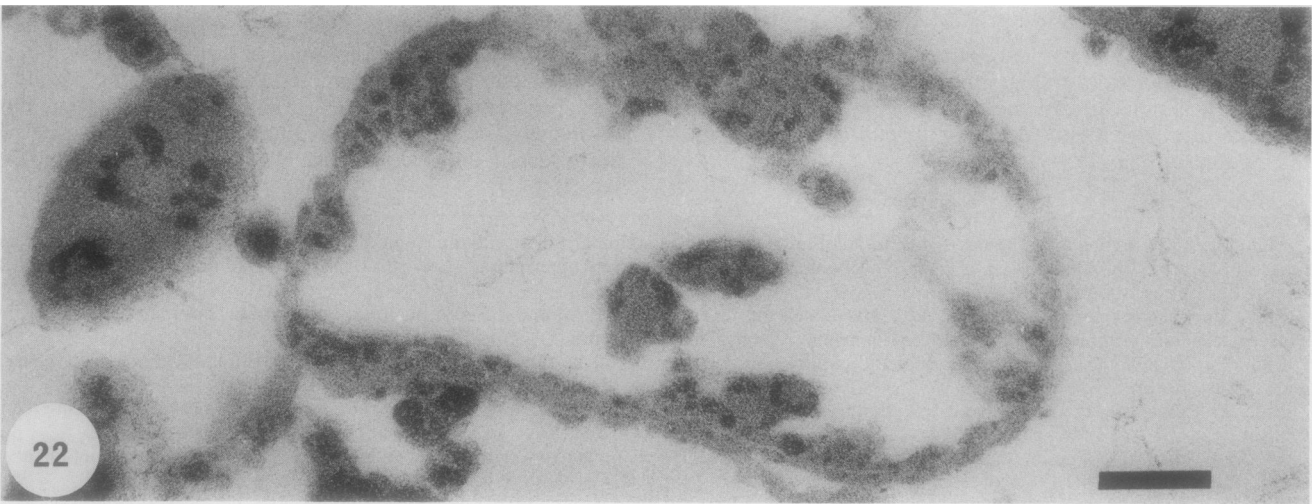
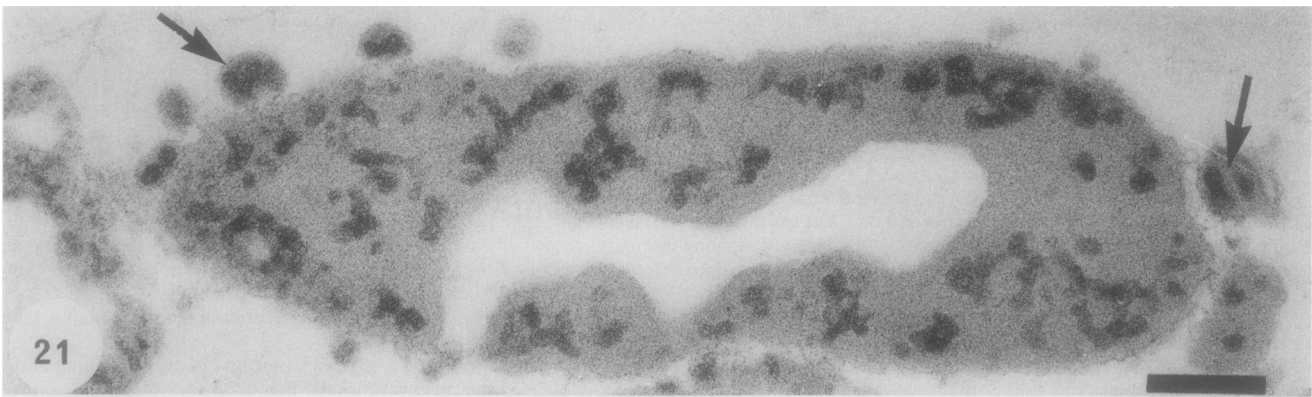
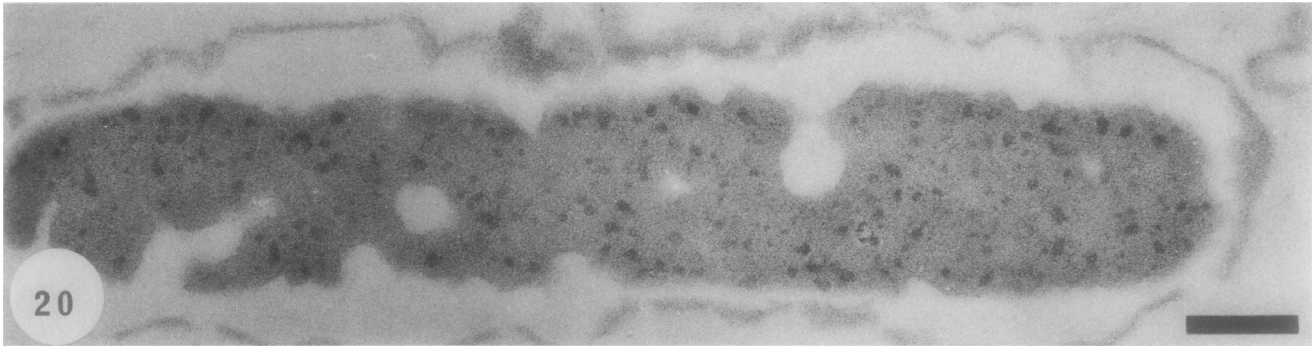
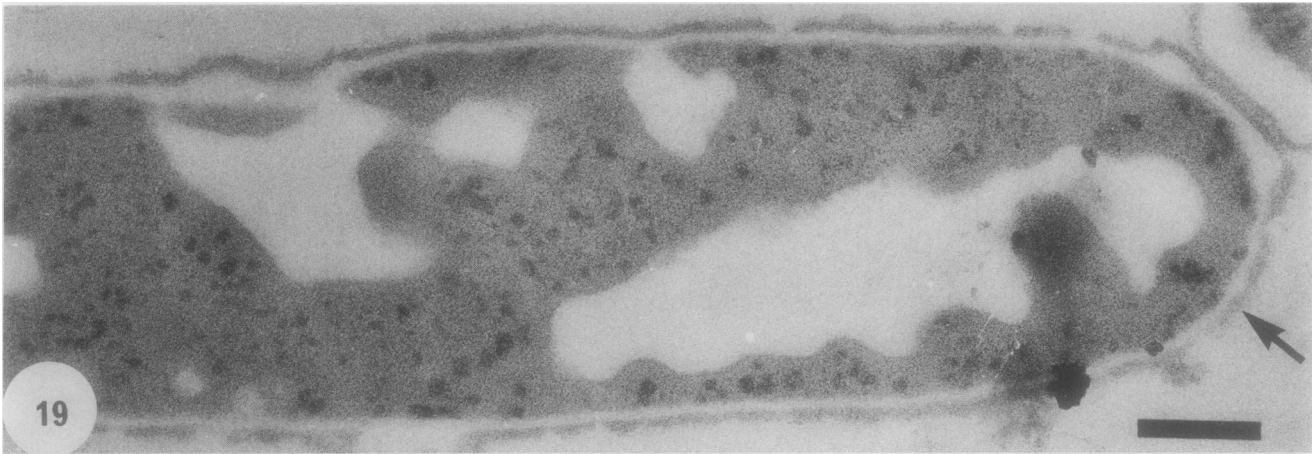
FIG. 11. Early-exponential-phase *B. fibrisolvens* cell that has been Gram stained, is gram positive, and contains copious amounts of the TPT-crystal violet complex (dark-staining cytoplasmic regions). Bar = 200 nm.

FIG. 12. Bright-field light micrograph of the culture used in Fig. 10 and 11. The cells are intensely stained and are gram positive. Cell diameter is 0.6 μ m.

FIG. 13. Same as Fig. 12 but from a stationary-phase culture. In this field of view, all of the cells are gram negative. Cell diameter is 0.6 μ m.

FIG. 14. Portion of a Gram-stained *B. fibrisolvens* cell that has lysed and is exuding cytoplasmic substance and TPT-crystal violet (arrow). Bar = 100 nm.

FIG. 15. Gram-stained stationary-phase *B. fibrisolvens* cell that is filled with cytoplasmic voids, contains little TPT-crystal violet complex, and as more complex departs, will stain gram negative as in Fig. 13. Bar = 100 nm.



increasing number of cells became sensitive to the decolorizing step of the Gram stain and their cell envelopes were breached, liberating cytoplasmic substance and the TPT-crystal violet complex (Fig. 14). These cells had large voids within them (Fig. 15). Eventually, electron microscopy showed these cells to be so devoid of the staining complex that they were gram negative.

Careful scrutiny of these growing cultures revealed that with time, the structure of the cell surface altered; the peptidoglycan layer became thinner as the cultures progressed from early to late exponential growth phase (cf. Fig. 17, 18, and Fig. 10 [inset]), so much so that its dimensions were reduced by half and it seemed incapable of withstanding the decolorization step. In fact, this wall layer was frequently not visible in those older cells that had been Gram stained (Fig. 19 to 22). In contrast to this layer, the outermost S layer was often visible and retained the shape of the cells (Fig. 19). As cultures approached the stationary growth phase, lesions were commonly seen in the S layer, and the protoplast had shrunk in size as if cytoplasmic substance had been lost (Fig. 20). Occasional cells had entirely lost their encompassing S layers and most of their substance (Fig. 21) and had rounded up (Fig. 16 [inset] and 22).

This entire set of observations (Table 2 and Fig. 10 to 22) suggested that bacteria in the *Bacillus-Butyrivibrio-Clostridium* group are gram variable because of a mechanism entirely different from that of the previous group. Although they have a more complex cell wall than do the others, the peptidoglycan-containing layer is thinner (cf. Fig. 2 with Fig. 10 and 16). This steady decrease in peptidoglycan thickness during growth coincided directly with the increased numbers of gram-negative cells. The very fragility of these cells made it impossible to detect whether septal sites were the most sensitive regions for cytoplasmic leakage; leakage occurred at a number of sites around the cell periphery.

It was interesting to note that as the peptidoglycan became fragile, the S layer was left to maintain cell shape. Yet as S-layered bacteria age, it is not uncommon that these surface arrays fragment and slough off the cell surface (1, 18, 21). This can occur at sites of division (20) or along the cylindrical wall (1, 21, 22) and may be a consequence of the insertion of new S layer (13, 16). The shedding of S layer is rarely, if ever, seen at the poles (13, 16). The results of this study are in agreement with these reports. As the bacteria used in this study aged and their peptidoglycan layer became thinner, presumably they relied more and more on their S layers for shape during Gram staining (Fig. 19). Yet the S layers would be shed as the cultures continued to age, and, during staining, cytoplasm would leak out until no shape was retained (Fig. 20 to 22). During this process, lesions in the S layers occurred along the cylindrical wall but were rarely encountered at the pole ends (Fig. 14, 19, and 20).

Gram variability. It would be impossible to cover the entire range of eubacteria that are unpredictable in their responses to the Gram stain. I have attempted to use a range of bacteria in this study that grow well in broth culture, that encompass a variety of genera, that have distinct growth

environments, and that (from my experience) are representative of gram-variable eubacteria. The ultrastructural approach combined with the TPT probe for the crystal violet staining complex has allowed these bacteria to be divided into two distinct groups.

As in our previous studies (4, 9) and the work of Salton (19), it is apparent that for eubacteria, the underlying principle of the Gram stain resides in the innate character of the cell wall. During staining, gram-positive bacteria such as *Micrococcus (lysodeikticus) luteus* stain intensely purple because their thick robust walls resist ethanol decolorization and the crystal violet-iodide complex is retained within the protoplast (19). The wall of *Escherichia coli* is so strongly affected by decolorization that the outer membrane is removed, the thin peptidoglycan layer is breached, and the crystal violet-iodide complex is removed to make these cells gram negative (4). These staining responses are clear-cut and unequivocal. In the study described here, even in those eubacteria that undergo erratic staining, the response to the dye is controlled by the cell wall. Indeed, two bacterial groups with distinctly different walls are defined by the degree of their gram variability. Members of the *Actinomyces-Arthrobacter-Corynebacterium-Mycobacterium-Propionibacterium* group are similar to most other gram-positive bacteria in that they have relatively thick and robust walls, but their initial septal sites do not appear to be as highly integrated into the side wall as in other varieties. This may indicate a common mode of septum initiation even though each genus within the group has subtle chemical differences to its wall fabric. Members of the *Bacillus-Butyrivibrio-Clostridium* group possess distinctly different walls. Each appears to have a reduced complement of peptidoglycan (i.e., a thinner peptidoglycan-containing layer) that is overlaid by an S layer. Initially, at low cell doubling rates, this combination of two layers is hardy enough to ensure that the cells stain gram positive. Yet with time, the peptidoglycan layer grows thinner and the cells become more prone to gram negativity. Each of these two gram-variable staining groups is distinct from the other in cell wall architecture, and each owes its particular brand of staining response to its wall design.

I must emphasize that these stain groupings by no means encompass the entire range of species within a given genus. For example, from my experience with a genus from the second staining group, *Bacillus subtilis*, *Bacillus megaterium*, and *Bacillus licheniformis* have thick cell walls (ca. 25 nm), do not possess S layers, and consistently stain gram positive until at least the late stationary phase or the induction of sporulation. Select strains of *Bacillus thuringiensis*, *Bacillus anthracis*, *Bacillus cereus*, and *Bacillus stearothermophilus* likewise have thick walls but also possess S layers; these cells consistently stain gram positive. *Bacillus polymyxa* and *Bacillus sphaericus* are more like *Bacillus brevis*; they have relatively thin walls plus S layers and are similarly gram variable. I must also emphasize that this study has used only representative eubacteria, and my experience with archaeobacteria and their unique surfaces suggests that subtly

FIG. 19 to 22. Series of micrographs of late-exponential-phase *Bacillus brevis* cells from the culture shown in the inset of Fig. 16. Some cells (Fig. 19) have a relatively intact S layer (arrow) and retain their rod shape. Others (Fig. 20) have fragmenting S layers, and their cytoplasm has reduced in size. Eventually, the S layer can no longer be seen (Fig. 21), portions of the cytoplasm are sloughing off into the external milieu (arrows), and only a spherical empty shell remains of the cell (Fig. 22). I believe that this progressive loss of shape and of cytoplasm accounts for the gradation of stain intensity seen in the inset of Fig. 16; gram negativity would increase from Fig. 19 to 22. Bar = 100 nm in all micrographs.

different staining mechanisms might be involved for archaeobacteria.

ACKNOWLEDGMENTS

I am grateful to M. D. Luckevich for help in the study during her tenure as a National Science and Engineering Research Council (NSERC) of Canada summer assistant in this laboratory and to J. A. Davies, University of Toledo, for synthesis of TPt.

This research was funded by a Medical Research Council of Canada operating grant to T.J.B. The NSERC Guelph Regional STEM Facility is partially maintained by an NSERC of Canada infrastructure grant to T.J.B.

LITERATURE CITED

1. Beveridge, T. J. 1981. Ultrastructure, chemistry, and function of the bacterial wall. *Int. Rev. Cytol.* **72**:229–317.
2. Beveridge, T. J. 1988. Wall ultrastructure: how little we know, p. 3–20. *In* P. Actor, L. Daneo-Moore, M. L. Higgins, M. R. J. Salton, and G. D. Shockman (ed.), *Antibiotic inhibition of bacterial cell surface assembly and function*. American Society for Microbiology, Washington, D.C.
3. Beveridge, T. J. 1988. The bacteria surface: general considerations towards design and function. *Can. J. Microbiol.* **34**:363–372.
4. Beveridge, T. J., and J. A. Davies. 1983. Cellular responses of *Bacillus subtilis* and *Escherichia coli* to the Gram stain. *J. Bacteriol.* **156**:846–858.
5. Burdett, I. D. J. 1980. Analysis of autolysis in *Bacillus subtilis* by electron microscopy. *J. Gen. Microbiol.* **120**:35–49.
6. Cheng, K.-J., and J. W. Costerton. 1977. Ultrastructure of *Butyrivibrio fibrisolvens*: a gram-positive bacterium? *J. Bacteriol.* **129**:1506–1512.
7. Chock, P. B., J. Halpern, and F. E. Paulik. 1973. Potassium trichloro(ethylene)platinate (II) (Zeisse's salt). *Inorg. Synth.* **14**:90–92.
8. Cummins, C. S., and J. L. Johnson. 1986. Genus I. *Propionibacterium* Orla-Jensen 1909, 337^{AL}, p. 1357. *In* P. H. A. Sneath (ed.), *Bergey's manual of systematic bacteriology*, vol. 2. The Williams & Wilkins Co., Baltimore.
9. Davies, J. A., G. K. Anderson, T. J. Beveridge, and H. C. Clark. 1983. Chemical mechanism of the Gram stain and synthesis of a new electron-opaque marker for electron microscopy which replaces the iodine mordant of the stain. *J. Bacteriol.* **156**:837–845.
10. Doyle, R. J., and A. L. Koch. 1987. The functions of autolysins in growth and division of *Bacillus subtilis*. *Crit. Rev. Microbiol.* **15**:169–222.
11. Drew, S. W. 1981. Liquid culture, p. 151–178. *In* P. Gerhardt, R. G. E. Murray, R. N. Costilow, E. W. Nester, W. A. Wood, N. R. Krieg, and G. B. Phillips (ed.), *Manual of methods for general bacteriology*. American Society for Microbiology, Washington, D.C.
12. Goodfellow, M., M. D. Collins, and D. E. Minnikin. 1976. Thin-layer chromatographic analysis of mycolic acid and other long-chain components in whole-organism methanolysates of coryneform and related taxa. *J. Gen. Microbiol.* **96**:351–358.
13. Gruber, K., and U. B. Sleytr. 1988. Localized insertion of new S-layer during growth of *Bacillus stearothermophilus* strains. *Arch. Microbiol.* **149**:485–491.
14. Higgins, M. L., J. Coyette, and G. D. Shockman. 1973. Sites of cellular autolysis in *Lactobacillus casei*. *J. Bacteriol.* **116**:1375–1382.
15. Higgins, M. L., and G. D. Shockman. 1971. Prokaryotic cell division with respect to wall and membranes. *Crit. Rev. Microbiol.* **1**:29–72.
16. Howard, L. V., D. D. Dalton, and W. K. McCouberty, Jr. 1982. Expansion of the tetragonally arrayed cell wall protein layer during growth of *Bacillus sphaericus*. *J. Bacteriol.* **149**:748–757.
17. Koch, A. L. 1981. Growth measurement, p. 179–207. *In* P. Gerhardt, R. G. E. Murray, R. N. Costilow, E. W. Nester, W. A. Wood, N. R. Krieg, and G. B. Phillips (ed.), *Manual of methods for general bacteriology*. American Society for Microbiology, Washington, D.C.
18. Luckevich, M. D., and T. J. Beveridge. 1989. Characterization of a dynamic S layer on *Bacillus thuringiensis*. *J. Bacteriol.* **171**:6656–6667.
19. Salton, M. R. J. 1963. The relationship between the nature of the cell wall and the Gram stain. *J. Gen. Microbiol.* **30**:223–235.
20. Sleytr, U. B., and A. M. Glauert. 1976. Ultrastructure of the cell walls of two closely related Clostridia that possess different regular arrays of surface subunits. *J. Bacteriol.* **126**:869–882.
21. Sleytr, U. B., and P. Messner. 1983. Crystalline surface layers on bacteria. *Annu. Rev. Microbiol.* **37**:311–339.
22. Sleytr, U. B., and P. Messner. 1988. Crystalline surface layers in prokaryotes. *J. Bacteriol.* **170**:2891–2897.